Temperature-dependent exciton linewidths in semiconductor quantum wells

S. Rudin
U.S. Army Electronics Technology and Devices Laboratory, Fort Monmouth, New Jersey 07703-5000

T. L. Reinecke
Naval Research Laboratory, Washington, D.C. 20375-5000
(Received 7 July 1989)

The temperature-dependent linewidth of excitons in semiconductor quantum wells due to the interaction of the exciton with LO phonons is studied with use of perturbation theory for the exciton-phonon interaction and by assuming an infinite-barrier-quantum-well model. The interaction is taken to be of the Fröhlich form, and the scattering of the exciton to both bound and scattering states of the interacting electron–heavy-hole system has been taken into account. The dependence of the linewidth on the quantum-well width and on the choice of the heavy-hole mass is discussed, and comparison is made with available experimental data. The effects of the confinement of the optical phonons on the exciton linewidth are also studied and are found not to alter substantively the results for the dependence of the linewidth on the quantum-well width.

I. INTRODUCTION

The optical properties of semiconductor heterostructures are of considerable interest for possible applications in optoelectronics.[1] Emission and absorption near the band gap in high-quality direct-band-gap semiconductors are dominated by excitonic features.[2] In GaAs/$Ga_{1-x}Al_xAs$ multiple quantum wells, excitons exist up to room temperature[3] and thus are especially interesting for possible applications.[4] The shape of these optical features is determined by the exciton linewidth. For the GaAs/$Ga_{1-x}Al_xAs$ system grown by molecular-beam epitaxy, a number of experimental results for the exciton linewidth has been reported based on optical absorption,[5,6] optical reflection,[7] and luminescence[6,8,9] studies.

The observed temperature dependence of the linewidth comes from the homogeneous broadening due to exciton-phonon interactions. The physical mechanism in the case of quantum wells is the same as that in bulk semiconductors with direct band gaps.[10,11] For weak exciton-phonon interaction the absorption, which is calculated from the imaginary part of the exciton Green's function, has a Lorentzian line shape with a half-width given by the imaginary part of the exciton self-energy evaluated at the exciton resonance frequency.[12,13] The exciton lifetime is related to its calculated linewidth through the energy uncertainty principle.

The contribution of the homogeneous broadening to the linewidth can be written in the form

$$\Gamma_{\rm hom}(T)=\sigma T+\gamma N_{\rm LO}(T)\ . \tag{1.1}$$

The first term on the right-hand side arises from exciton interactions with acoustic phonons. The second term arises from interactions with longitudinal-optical (LO) phonons, and it is proportional to the phonon population function $N_{\rm LO}(T)$. This form of the temperature dependence assumes dispersionless bulk LO phonons and will be modified by the effect of the multiple-quantum-well system on the optical phonons, as shall be discussed later.

In this work we present a detailed study of the LO-phonon contribution to the temperature-dependent linewidth arising from a process which involves the absorption of a LO phonon accompanied by the exciton being scattered to a bound or to a continuum state.[11] In general, scattering to all energetically accessible intermediate states should be taken into account. In this work we use an infinite-barrier quantum-well model and the effective-mass approximation to study the dependence of the linewidth parameter γ on the quantum-well width L. We also discuss the dependence of the results on the choice of heavy-hole mass for the nonparabolic valence bands. The importance of the contribution from the continuum states to the linewidth in bulk semiconductors was pointed out previously.[10,11] In this work, we treat the continuum states as scattering states of the interacting electron-hole pair. In this respect our calculations of Γ significantly differ from other recent theoretical treatments.[9,14]

A brief version of these results was given in a previous publication.[15] There the phonons were assumed to be three-dimensional bulk modes, and the resulting linewidth Γ depended on confinement through the electron-hole wave function. The interaction was assumed to be of the Fröhlich form. In the present paper we provide the details of the calculations, and we investigate how the confinement of the optical phonons affects the calculated values for the exciton linewidth. In the present work we shall not include "polariton effect" in the linewidth calculations. This effect gives a modification in the linewidth due to the strong resonant coupling of the light and the exciton. In the bulk case we

discussed this effect and showed that it resulted in a reduction of Γ.[11] This reduction, however, was not as significant as the reduction we used previously[15] and it will not be included here. Some relevant discussion of this point is given at the end of Sec. IV. We also note that the more detailed treatment of all relevant contributions to the linewidth given here makes its dependence on the well width L at small values of L more pronounced than given previously.[15] This, however, is further modified by the effects of phonon confinement as discussed in Sec. V.

The calculational scheme for γ follows closely the one employed previously for the bulk case.[11] For the quantum-well case considered here we assume that both the electron and the heavy hole are confined in the first subband of their corresponding wells.[16] The exciton states then will be characterized by the in-plane two-dimensional wave vector and by the internal state of the exciton. The exciton self-energy is calculated to the lowest order in the exciton-phonon interaction (the Fröhlich interaction can be treated as weak for GaAs as shown in Ref. 11). Thus, for the exciton initially in a ground state only, 1-LO-phonon transitions are involved. From our results for the bulk case[11] and from the exact results for the two-dimensional limit given here (see below) we know that the dominant contribution to γ is obtained from the scattering of the exciton to the continuum states of the interacting electron-hole pair. In the present work scattering to the exciton ground state (the intraband contribution) and to continuum states (the dominant part of the interband contribution) will be taken into account by employing variational wave functions for the ground state[16] and two-dimensional (2D) Coulomb wave functions for the scattering states. These calculations assume spherical parabolic carrier bands, and we estimate the uncertainty in the values of the exciton mass by studying the dependence of γ on the choice of the heavy-hole mass. To investigate the effects of phonon confinement on Γ we calculate both intraband and interband contributions as functions of the well width L where both the exciton and the optical phonons are taken to be confined modes.

This paper is organized as follows. In Sec. II the basic formalism for the linewidth contribution from the exciton–LO-phonon interaction in the presence of confining potentials is given. The strictly 2D exciton limit, for which all the contributions to γ can be summed exactly, is considered in detail in Sec. III. In Sec. IV we employ variational wave functions for the ground state and 2D scattering states to calculate the dependence of the linewidth parameter γ on the quantum-well width L, and the results are compared with the available experimental data.[5–8] In Sec. V we calculate linewidth $\Gamma(T)$ taking the effects of the confinement of the optical phonons into account. In this calculation the interactions of the exciton with the interface modes and with the bulk-like confined modes are included, and different approximations for "confined bulk modes" are discussed. Several lengthy expressions that appear in the results for the linewidth in Secs. III and IV are given in the Appendix.

II. QUANTUM-WELL EXCITONS AND THE EXCITON LINEWIDTH DUE TO INTERACTION WITH LO PHONONS

A general electron-hole state can be written as

$$|\Psi_{\rm ex}\rangle=\sum_{\mathbf{k},\mathbf{k}'}F(\mathbf{k},\mathbf{k}')c_{\mathbf{k}}^{\dagger}d_{\mathbf{k}'}^{\dagger}|G\rangle\ , \tag{2.1}$$

where $|G\rangle$ is the ground state of the semiconductor, $c^{\dagger}$ and $d^{\dagger}$ are the electron and hole creation operators, and $\mathbf{k}$ is the 3D wave vector. The electron-hole wave function in real space is defined by the Fourier transformation of $F(\mathbf{k},\mathbf{k}')$:

$$\Psi(\mathbf{x}_e,\mathbf{x}_h)=\sum_{\mathbf{k},\mathbf{k}'}F(\mathbf{k},\mathbf{k}')\exp(i\mathbf{k}\cdot\mathbf{x}_e-i\mathbf{k}'\cdot\mathbf{x}_h)\ . \tag{2.2}$$

In the effective-mass approximation[17,18] for the exciton in the quantum-well potentials $W_e(x_e), W_h(x_h)$, one obtains the Schrödinger equation

$$\left[-\frac{\hbar^2}{2m_e}\nabla_e^2-\frac{\hbar^2}{2m_h}\nabla_h^2+W_e(\mathbf{x}_e)-W_h(\mathbf{x}_h)-\frac{e^2}{\epsilon_0}|\mathbf{x}_e-\mathbf{x}_h|^{-1}\right]\Psi(\mathbf{x}_e,\mathbf{x}_h)=(E-E_g)\Psi(\mathbf{x}_e,\mathbf{x}_h)\ , \tag{2.3}$$

where E_g is an energy gap, and m_e and m_h are masses of the electron and heavy-hole obtained from the band structure near the origin in $\mathbf{k}$ space.

We use the Coulomb interaction screened by the static dielectric constant ϵ_0 of the quantum-well material. This form results from the screening by the bound electrons[19,20] giving $-e^2/\epsilon_\infty r$ and a contribution from the LO phonons of $(e^2/r)(1/\epsilon_\infty-1/\epsilon_0)$. This approximation is valid in the large-exciton limit. The criterion for the validity of a large-exciton approximation in this case is $E_B<\hbar\omega_{\rm LO}$, where E_B is the binding energy and $\omega_{\rm LO}$ is the LO-phonon frequency. We do not include the effects of the image charges from the barrier material.[21]

The pair-creation operator[22] is defined as

$$B^{\dagger}(\mathbf{x}_e,\mathbf{x}_h)=V^{-1}\sum_{\mathbf{k},\mathbf{k}'}\exp(-i\mathbf{k}\cdot\mathbf{x}_e-i\mathbf{k}'\cdot\mathbf{x}_h)c_k^{\dagger}d_{k'}^{\dagger}\ . \tag{2.4}$$

In the exciton subspace of the electron-hole-phonon Hilbert space we can rewrite the carrier-phonon Hamiltonian in terms of the exciton operators[22] defined as

$$B_{\lambda q}^{\dagger}=\int d^3x_e\int d^3x_h\,\Psi_{\lambda q}(\mathbf{x}_e,\mathbf{x}_h)B^{\dagger}(\mathbf{x}_e,\mathbf{x}_h)\ , \tag{2.5}$$

where q,λ is a set of quantum numbers which distinguishes between the solutions of Eq. (2.3). At low exciton density excitons can be treated as bosons,[22]

$$[B_{\lambda q},B_{\lambda' q'}^{\dagger}]=\delta_{\lambda\lambda'}\delta_{qq'}+O(n_{\rm ex})\ . \tag{2.6}$$

Because the motion in the plane of the quantum well is translationally invariant, we transform the in-plane coordinates to the in-plane center-of-mass (c.m.) system and separate the c.m. motion from the relative motion of the electron and hole,

$$\mathbf{x}_e,\mathbf{x}_h\rightarrow\mathbf{r},\mathbf{R},z_e,z_h\ , \tag{2.7}$$

where $\mathbf{r}$ and $\mathbf{R}$ are 2D vectors referring to the relative and c.m. motion, respectively, and the Jacobian of the transformation is unity.

Then,

$$\Psi(\mathbf{x}_e,\mathbf{x}_h)=A^{-1/2}\exp(i\mathbf{q}\cdot\mathbf{R})\Phi(\mathbf{r},z_e,z_h)\ , \tag{2.8}$$

where A is area and $\Phi(\mathbf{r},z_e,z_h)$ satisfies the usual envelope-function equation for the motion of the exciton in a quantum well,[16]

$$\left[-\frac{\hbar^2}{2m_e}\frac{\partial^2}{\partial z_e^2}-\frac{\hbar^2}{2m_h}\frac{\partial^2}{\partial z_h^2}-W_e(z_e)-W_h(z_h)-\frac{\hbar^2}{2\mu}\nabla_r^2 -\frac{e^2}{\epsilon_0}[r^2+(z_e-z_h)^2]^{-1/2}\right]\Phi(\mathbf{r},z_e,z_h) =\left[E-E_g-\frac{\hbar^2q^2}{2M}\right]\Phi(r,z_e,z_h)\ , \tag{2.9}$$

where μ is the exciton reduced mass defined by $\mu^{-1}=m_e^{-1}-m_h^{-1}$. With Eqs. (2.1)–(2.4) we can now rewrite the electron-hole–phonon Hamiltonian,

$$H_{\rm ex}=\sum_{\lambda,q}E_{\lambda q}B_\lambda^\dagger(\mathbf{q})B_\lambda(\mathbf{q})\ , \tag{2.10}$$

$$H_{\rm ph}=\sum_{\mathbf{Q}}\hbar\omega_Q a^\dagger(\mathbf{Q})a(\mathbf{Q})\ , \tag{2.11}$$

$$H_{\text{ex-ph}}=\sum_{\lambda,\lambda',\mathbf{k},\mathbf{Q}}V^{\lambda\lambda'}(q)B_\lambda^\dagger(\mathbf{k}+\mathbf{q})B_{\lambda'}(\mathbf{k}) \times[a(\mathbf{Q})+a^\dagger(-\mathbf{Q})]\ , \tag{2.12}$$

where $\mathbf{q}$ is the 2D component of the 3D vector $\mathbf{Q}=(\mathbf{q},q_z)$, and the optical phonons are treated as three dimensional.

The interaction matrix element can be written as[15]

$$V^{\lambda\lambda'}(\mathbf{Q})=u_Q\int d^2r\int dz_e\int dz_h\,\Phi_\lambda^*(\mathbf{r},z_e,z_h)\Phi_{\lambda'}(\mathbf{r},z_e,z_h)\ [\exp(i\mathbf{q}\cdot\mathbf{r}m_h/M+iq_zz_e)-\exp(-i\mathbf{q}\cdot\mathbf{r}m_e/M+iq_zz_h)]\ , \tag{2.13}$$

where u_Q for a Fröhlich interaction is given by

$$u_Q=[2\pi e^2\hbar\omega_{\rm LO}(\epsilon_\infty^{-1}-\epsilon_0^{-1})V^{-1}]^{1/2}Q^{-1} \tag{2.14}$$

and $M=m_e+m_h$ is the total mass of the exciton.

For convenience we introduce the notation $V^{\lambda\lambda'}(Q)=u_Q v_{\lambda\lambda'}(Q)$.

Just as in a bulk case,[10,11] if the exciton self-energy is evaluated to the lowest order in perturbation theory, we obtain for the half-width of the lowest ($1s$) exciton state

$$\Gamma_{1s}(T)=N_{\rm LO}(T)(e^2\hbar\omega_{\rm LO}/4\pi)(\epsilon_\infty^{-1}-\epsilon_0^{-1}) \times\int d^3Q\sum_\lambda Q^{-2}|v_{\lambda,1s}(Q)|^2 \times\delta(\hbar\omega_{1s}-E_\lambda(q)+\hbar\omega_{\rm LO})\ , \tag{2.15}$$

where $N_{\rm LO}(T)=[\exp(\hbar\omega_{\rm LO}/k_BT)-1]^{-1}$ is the Bose function of thermal phonons.

The objective of the present work is to evaluate Eq. (2.15) taking into account all energetically available states within first subband in an infinite-potential approximation for the quantum well. Before evaluating Eq. (2.15) for a quantum well of finite width, we consider the $L\to0$ limit, i.e., the strictly two-dimensional case.

III. LINEWIDTH OF THE EXCITON IN TWO DIMENSIONS

The 2D limit of Eq. (2.15) is obtained by integrating over all values of the z component of the wave vector $\mathbf{Q}$ and then taking $L\to0$. Then integrating over the 2D wave vector $\mathbf{q}$ we obtain

$$\gamma_{1s}^{\rm 2D}=(\pi CM/2\hbar^2)\sum_\lambda q_\lambda^{-1}|v_{1s,\lambda}(q_\lambda)|^2\ , \tag{3.1}$$

where

$$C=e^2\hbar\omega_{\rm LO}(\epsilon_\infty^{-1}-\epsilon_0^{-1})\ , \tag{3.2}$$

and q_λ is given by

$$\hbar^2q_\lambda^2/2M=\hbar\omega_{\rm LO}+E_{1s}-E_\lambda\ . \tag{3.3}$$

$v_{1s,\lambda}$ is given in two dimensions by

$$v_{1s,\lambda}(q_\lambda)=\int d^2r\,\Phi_{1s}^*(\mathbf{r})\Phi_\lambda(\mathbf{r}) \times[\exp(i\mathbf{q}\cdot\mathbf{r}m_h/M) -\exp(-i\mathbf{q}\cdot\mathbf{r}m_e/M)]\ , \tag{3.4}$$

where $\Phi_\lambda(\mathbf{r})$ is an eigenfunction of the 2D Coulomb equation.

We redefine E_λ by choosing the zero of energy at the bottom of the conduction band so that for the discrete part of the spectrum $-E_\lambda$ is the exciton binding energy. The 2D Coulomb equation is then

$$\left[-\frac{\hbar^2}{2\mu}\nabla_r^2-\frac{e^2}{\epsilon_0 r}\right]\Phi_\lambda(\mathbf{r})=E_\lambda\Phi_\lambda(\mathbf{r})\ . \tag{3.5}$$

It is well known that the Coulomb problem has higher symmetry than that of a general spherical potential and allows separation in parabolic coordinates.[23,24] In the bulk case[11] we found that the use of the parabolic coordinates greatly simplifies the calculations involving the continuum part of the spectrum. Here we employ 2D parabolic coordinates[23] ξ,η defined by

$$x=\mathrm{sgn}\xi(|\xi|\eta)^{1/2},\quad y=(|\xi|-\eta)/2\ ,\quad -\infty<\xi<\infty,\quad 0<\eta<\infty,\quad r=(|\xi|+\eta)/2\ . \tag{3.6}$$

By choosing the y axis along $\mathbf{q}$, we separate the ξ and η integrations in Eq. (3.4).

We can consider solutions of the Schrödinger equation

(3.5) first in the region $\xi>0$, and then extend them by the continuity of $\Phi(\mathbf{r})$ and $\nabla_r\Phi(\mathbf{r})$ to the region $\xi<0$. The separation of variables $\Phi(\xi,\eta)=f_1(\xi)f_2(\eta)$ in a positive-ξ region gives

$$\xi f_1''+f_1'/2+(\sigma_1+\xi\Omega/4)f_1=0\ , \tag{3.7}$$

$$\eta f_2''+f_2'/2+(\sigma_2+\eta\Omega/4)f_2=0\ , \tag{3.8}$$

where

$$\Omega=2\mu E/\hbar^2 \tag{3.9}$$

and the separation constants are related through

$$\sigma_1+\sigma_2=e^2\mu/\hbar^2\epsilon_0\ . \tag{3.10}$$

General solutions for f_1 and f_2 are given by the linear combinations of confluent hypergeometric functions.[23] We now consider the bound- and scattering-state solutions separately.

A. Bound states ($\Omega<0$)

The requirement that $\Phi(\xi,\eta)<\infty$ at infinity restricts solutions to finite polynomials, and defining

$$p=\sqrt{-\Omega} \tag{3.11}$$

we obtain in terms of Jacobi polynomials[23,24]

$$\Phi^e_{nn_1}(\xi,\eta)=N_{nn_1}\exp[-(|\xi|+\eta)p_n/2]\times F(-n_1,\tfrac{1}{2},|\xi|p_n)F(-n_2,\tfrac{1}{2},\eta p_n)\ , \tag{3.12}$$

$$n=0,1,2,\ldots;\quad n_1=0,1,\ldots,n\ ,\quad n_1+n_2=n\ , \tag{3.13}$$

$$\Phi^o_{nn_1}(\xi,\eta)=N'_{nn_1}\exp[-(|\xi|+\eta)p_n/2](\mathrm{sgn}\xi)\times(|\xi|\eta p_n^2)^{1/2}F(-n_1,\tfrac{3}{2},|\xi|p_n)\times F(-n_2,\tfrac{3}{2},\eta p_n)\ , \tag{3.14}$$

$$n=1,2,\ldots;\quad n_1=0,1,\ldots,n-1\ , \tag{3.15}$$

where

$$p_n=p_0/(2n+1)\ , \tag{3.16}$$

$$1/p_0=a=\hbar^2\epsilon_0/2e^2\mu\ . \tag{3.17}$$

Here N_{nn_1} and N'_{nn_1} are normalization constants which are calculated below.

These solutions have definite parity in ξ:

$$\Phi^{e,o}(\xi)=\pm\Phi^{e,o}(-\xi)\ . \tag{3.18}$$

They are normalized as

$$\langle\Phi^a_{nn_1}|\Phi^b_{mm_1}\rangle=\delta_{ab}\delta_{nm}\delta_{n_1m_1}\ . \tag{3.19}$$

The energy eigenvalues are given by

$$E_n=-R/(n+\tfrac{1}{2})^2\ , \tag{3.20}$$

where R is the effective Rydberg of the bulk material,

$$R=\mu e^4/2\hbar^2\epsilon_0\ . \tag{3.21}$$

The ground-state wave function is given by

$$\Phi^e_{00}=N_{00}\exp[-(|\xi|+\eta)p_0/2]\ . \tag{3.22}$$

B. Scattering states ($\Omega>0$)

For positive energies the spectrum is continuous and we normalize the eigenfunctions on the δ function.[24] We define a positive energy number k by

$$E=\hbar^2k^2/2\mu\ . \tag{3.23}$$

The continuity of the wave functions and their normalizability on the δ function restrict solutions for $\Omega>0$ to the following:

$$G^e_{k\beta}(\xi,\eta)=N_{k\beta}\exp[-i(|\xi|+\eta)k/2]\times F(i\beta_1/2ak+\tfrac{1}{4},\tfrac{1}{2},i|\xi|k)\times F(i\beta_2/2ak+\tfrac{1}{4},\tfrac{1}{2},i\eta k)\ , \tag{3.24}$$

$$G^o_{k\beta}(\xi,\eta)=N'_{k\beta}\exp[-i(|\xi|+\eta)k/2]\times(\mathrm{sgn}\xi)|\xi\eta k^2|^{1/2}F(i\beta_1/2ak+\tfrac{1}{4},\tfrac{1}{2},i|\xi|k)\times F(i\beta_2/2ak+\tfrac{1}{4},\tfrac{1}{2},i\eta k)\ , \tag{3.25}$$

where β_1 and β_2 are real numbers related through

$$\beta_1+\beta_2=1,\quad -\infty<\beta_1<\infty \tag{3.26}$$

and the solutions are normalized as

$$\langle G_{k\beta}|G_{k\beta}\rangle=\delta(k-k')\delta(\beta-\beta')\ . \tag{3.27}$$

The functions Φ_{nn_1} and $G_{k\beta}$ are to be used in Eqs. (3.1) and (3.4) to calculate matrix elements of the form

$$v_i=\langle\Phi_{00}|\exp(i\mathbf{Q}_i\cdot\mathbf{r})|\Phi(\xi,\eta)\rangle\ , \tag{3.28}$$

where $\Phi(\xi,\eta)$ is either $\Phi^{e,o}_{nn_1}$ or $G^{e,o}_{k\beta}$ and $\mathbf{Q}_i$ are defined for the electron and the hole as

$$\mathbf{Q}_h=qm_\lambda/M,\quad \mathbf{Q}_e=-qm_e/M\ . \tag{3.29}$$

Choosing the y axis along Q we rewrite Eq. (3.30) as

$$v_i=\langle\Phi_{00}|\exp[iQ_i(|\xi|-\eta)/2]|\Phi(\xi,\eta)\rangle\ , \tag{3.30}$$

and thus $v_i=0$ for the odd functions Φ^o and G^o. Hence only the functions even in ξ are needed for the evaluation of γ_{1s} in Eq. (3.1).

The normalization factor in Eq. (3.12) is easily obtained by integrating products of hypergeometric functions:[24]

$$N_{nn_1}=a^{-1}\pi^{-1/2}2^{-n/2+1/2}(2n+1)^{-3/2}\times[(2n_1-1)!!\,(2n_2-1)!!/(n_1!\,n_2!)]^{1/2}\ . \tag{3.31}$$

The normalization factor in Eq. (3.24) is obtained in a same way as we have done in the 3D case[11] by integrating Eq. (3.27) over small intervals $\Delta k,\Delta\beta$ and then using asymptotic expressions for hypergeometric functions. In this way an exact value of N is obtained:

$$N_{k\beta}=(1/4\pi^2)a^{-1/2}\exp(\pi/4ak)\times|\Gamma(i\beta_1/2ak+\tfrac{1}{4})\Gamma(i\beta_2/2ak+\tfrac{1}{4})|\ , \tag{3.32}$$

where Γ is the gamma function.

Separating in Eq. (3.1) contributions of the final states belonging to the discrete and continuum parts of the spectrum, we write

$$\gamma^{2D}=\gamma^{2D}_{1s,\text{disc}}+\gamma^{2D}_{1s,\text{cont}} . \tag{3.33}$$

We substitute (3.12) and (3.31) in Eq. (3.4) to obtain, for the contribution of the bound final states, the following expression:

$$\gamma^{2D}_{1s,\text{disc}}=(\pi/2)(M/\mu)\hbar\omega_{\text{LO}}(\epsilon_0/\epsilon_\infty-1) \times\sum_{n=0}^{\infty}\sum_{n_1=0}^{n}\Delta(n,n_1) . \tag{3.34}$$

The lengthy expression for $\Delta(n,n_1)$ is given in the Appendix. The summation over n in Eq. (3.34) has an upper limit of ∞ if $\hbar\omega_{\text{LO}}>B_1$, where B_1 is a binding energy of the exciton's ground state. Because this is the case for GaAs, we have used that upper limit in Eq. (3.34).

Next we substitute (3.24) and (3.32) into Eq. (3.4) and obtain after some lengthy integrations, including integration over β, the following expression for the contribution of the scattering final states:

$$\gamma^{2D}_{1s,\text{cont}}=4\pi\hbar\omega_{\text{LO}}(M/\mu)^{1/2}(\epsilon_0/\epsilon_\infty-1) \times\int_0^{x_0}dx\, x[1+\exp(-\pi/x)]^{-1} \times(F_{ee}+F_{hh}-2F_{eh}) . \tag{3.35}$$

The functions F_{ee}, F_{hh}, and F_{eh} are given in the Appendix. The upper limit of the integration is derived from the energy-conservation equation and is given by $x_0=0.5(\mu/m_0)\epsilon_0[(\omega_{\text{LO}}\hbar-B_1)/R_0]$, where $R_0=13\,605.8$ meV is the usual Rydberg constant, B_1 is the binding energy of the $1s$ state, and m_0 is the vacuum electron mass. The evaluation of F_{eh} in the integrand involves numerical integration as explained in the Appendix, and the overall integration in Eq. (3.35) is also performed numerically.

We have fitted calculations[25] of the dispersion of the heavy-hole valence band for finite quantum wells grown along the [100] direction and obtained mass values in the range $m_h/m_0=0.15$–0.18 for varying well widths. For the 2D case we show in Table I the results of the contributions to the linewidth parameter γ^{2D}_{1s} from the intraband transitions $(1s,1s)$, transitions to all higher-lying excited bound states $(1s,\text{eb})$ and continuum states $(1s,c)$ for various choices of m_h/m_0. The following values of the parameters for GaAs were used here and are used in the next section: $m_e=0.0665m_0$, $\hbar\omega_{\text{LO}}=36.8$ meV, $\epsilon_0=12.35$, $\epsilon_\infty=10.48$. We see that the total γ^{2D}_{1s} is considerably less sensitive to variations in m_h than are the separate $(1s,1s)$ and $(1s,c)$ contributions. In the next section, dealing with the finite-width quantum well, we investigate the dependence of the linewidth on the well width L. The $L\to0$ results given in Table I indicate that for smaller values of the heavy-hole mass the transitions to the continuum give the dominant contribution to γ_{1s}.

TABLE I. Contributions of bound and continuum exciton states to the 2D limit of the linewidth parameter γ_{1s} for several values of the heavy-hole mass m_h. $\gamma^{2D}_{1s,1s}$ is a contribution of the intraband $(1s,1s)$ transition, $\gamma^{2D}_{1s,\text{eb}}$ is a contribution of the excited bound states others than $1s$, $\gamma^{2D}_{1s,\text{cont}}$ is a contribution of all scattering states, and γ^{2D}_{1s} is a total value.

m_h/m_0	$\gamma^{2D}_{1s,1s}$	$\gamma^{2D}_{1s,\text{eb}}$	$\gamma^{2D}_{1s,\text{cont}}$	γ^{2D}_{1s}
0.15	1.33	0.87	8.51	10.71
0.2	2.45	0.90	5.24	8.59
0.3	4.50	0.85	3.50	8.85
0.5	7.85	0.66	2.41	10.92

IV. EXCITON LINEWIDTH IN A QUANTUM WELL

For a quantum well of finite width L we approximate γ as

$$\gamma_{1s}\approx\gamma_{1s,1s}+\gamma_{1s,\text{cont}} . \tag{4.1}$$

From the results for the two-dimensional case in the previous section and the results for the bulk case,[11] we believe that the contributions from the transitions to the higher-lying bound states are small, and thus Eq. (4.1) provides a good approximation for γ_{1s}. In addition, only the first quantum-well subband for the confined electron and hole will be taken into account. This will restrict the applicability of our calculations to $L<200$ Å. To evaluate $\gamma_{1s,1s}$, we employ a variational wave function[16,26] which correctly reproduces the 2D and 3D limits. To evaluate $\gamma_{1s,\text{cont}}$ we use a separable variational wave function for the ground state; we also use the two-dimensional scattering states of the previous section, but with the parameter a in Eq. (3.24) chosen to be the same as for the ground-state variational wave function so that these scattering states are orthogonal to the variational ground state.

A. Contribution of the ground state

We choose a variational wave function of the form

$$\Phi_{1s}(\mathbf{r},z_e,z_h)=N_\alpha f(z_e)f(z_h) \times\exp\{-(\alpha/2)[r^2+(z_e-z_h)^2]^{1/2}\} , \tag{4.2}$$

where we use envelope functions appropriate for an infinite-well potential

$$f(z)=\cos(\pi z/L),\quad |z|<L/2 . \tag{4.3}$$

Parameter α is to be determined variationally by minimizing the energy expectation value,[23] and N_α is a normalization constant which depends on α and L.

We substitute Eq. (4.2) in Eqs. (2.13) and (2.15), and after some calculation we obtain $\gamma_{1s,1s}$ in the form of the following integral:

$$\gamma_{1s,1s}=(8CM/\hbar^2)\alpha^2N_\alpha^4 \times\int_{-\infty}^{\infty}dx(x^2+q_1^2)^{-1}[J_e(x)-J_h(x)]^2 , \tag{4.4}$$

where C is defined by Eq. (3.2) and q_1 is given by Eq. (3.3) with $\lambda=1$. The functions $I_e(x), I_h(x)$ are defined by

$$I_i(x)=\int_{-\infty}^{\infty} dy\, F(x+y)F(y)(y^2+u^2)^{-2}\ , \tag{4.5}$$

where

$$u=(Q^2+\alpha^2)^{1/2}\ . \tag{4.6}$$

Q_i is given in (3.31), and

$$F(x)=\int_{-\infty}^{\infty} dz\, f(z)f^*(z)\exp(izx)\ . \tag{4.7}$$

Equation (4.5) can be evaluated in terms of elementary functions, and then we are left with only one integration in Eq. (4.4) to be performed numerically. The expression for N_α also has been evaluated in terms of elementary functions.

B. Contribution of the scattering states

To make the evaluation of $\gamma_{1s,\mathrm{cont}}$ feasible we use a separable variational wave function for the ground state in Eq. (2.13),

$$\Psi_{1s}(\mathbf{r},z_e,z_h)=N'_\alpha f(z_e)f(z_h)\exp(-\alpha r/2)\ , \tag{4.8}$$

where $f(z)$ is given by Eq. (4.3).

The scattering states are approximated by the quasi-two-dimensional form

$$\Psi_c(\mathbf{r},z,z)=(2\pi/L)f(z_e)f(z_h)G(\mathbf{r})\ , \tag{4.9}$$

where $\mathbf{r}$ is the in-plane 2D vector, and $G(\mathbf{r})$ in parabolic coordinates is given by Eq. (3.24) with an L-dependent parameter a representing the exciton radius in a quantum well:

$$a(L)=2/\alpha(L)\ . \tag{4.10}$$

Here α is the same variational parameter as in Eq. (4.8). Then Ψ_c is orthogonal to Ψ_{1s}:

$$\langle\Psi_{1s}|\Psi_c\rangle=0 \tag{4.11}$$

The resulting expression for $\gamma_{1s,\mathrm{cont}}$ then can be written in a form similar to that for the 2D case in Eq. (3.3):

$$\gamma_{1s,\mathrm{cont}}=4\hbar\omega_{\mathrm{LO}}(M/\mu)^{1/2}(\epsilon_0/\epsilon_\infty-1)(a/a_0)\int_0^{x_0} dx\, g_L(x)x[1+\exp(-\pi/x)]^{-1}(F_{ee}^L+F_{hh}^L-2F_{eh}^L)\ , \tag{4.12}$$

where

$$g_L(x)=(4\pi a^2/L^2)x_1\{(L/2a)[x_1^{-2}+0.5(x_1^2+v^2)^{-1}]$$
$$+[1-\exp(-Lx_1/a)][-0.5x_1^{-3}+x_1^{-1}(x_1+v^2)^{-1}-0.5x_1(x_1^2+v^2)^{-2}]\}\ , \tag{4.13}$$

$$x_1=(M/\mu)^{1/2}(x_0^2-x^2)^{1/2}\ , \tag{4.14}$$

and $v=2\pi a/L$.

The upper limit in the integral in Eq. (4.12) is given by

$$x_0=0.5(\mu/m_0)^{-1/2}\epsilon_0[(\omega_{\mathrm{LO}}\hbar-B_1)/R_0]^{1/2}\ , \tag{4.15}$$

where now B_1 is the binding energy for the variational ground state of Eq. (4.8), $R_0=13\,605.8$ meV, $a_0=\hbar\epsilon_0/e^2\mu$, and a is $a(L)$ given in Eq. (4.10) above. The functions F_{ee}, F_{hh}, and F_{eh} are of the same form as those given in the Appendix, but with the parameter a replaced by $a(L)$ from Eq. (4.10).

The results for $\gamma(L)$ given by Eq. (4.1) are shown in Fig. 1 as a function of the well width L for three different values of the heavy-hole effective mass m_h. The value $m_h/m_0=0.15$ represents the best choice of a single heavy-hole mass for $L=100$–150 Å which was obtained by fitting the valence-band dispersion for small in-plane wave vector[25] as mentioned at the end of Sec. III. Results for $m_h/m_0=0.2$ and 0.3 are also shown[27] in order to provide a measure of the possible uncertainty in the linewidth arising from the nonparabolicity of the valence band at larger wave vectors.

In this section the phonons were assumed to be bulk GaAs LO modes unaffected by the compositional variations of the quantum-well system. In the next section we shall see how phonon confinement affects $\Gamma(T)$. As discussed in the next section, there exist several simple models to describe these confinement effects. We find that the results for Γ vary by a factor of 2 depending on the choice of model. The results for the exciton lifetimes which were obtained from what we believe to be the best

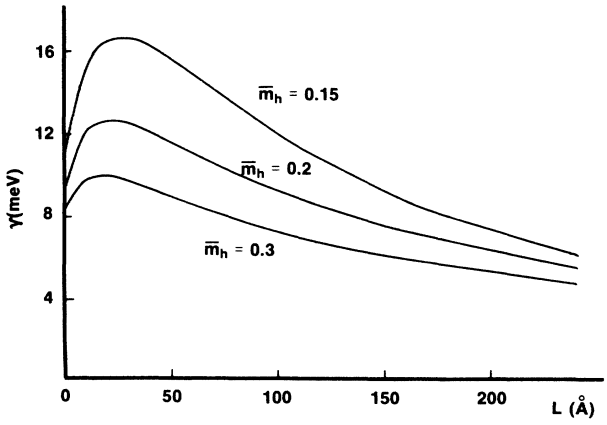

FIG. 1. Results obtained here from Eq. (4.1) for the LO-induced linewidth coefficient γ for excitons in a quantum well as a function of well width L for several choices of the heavy-hole mass $\bar{m}_h=m_h/m_0$. These results are obtained using a three-dimensional description of LO phonons of the bulk GaAs.

choice of model for the multiple-quantum-well phonons are fairly close to the ones obtained in this section based on a bulk LO-phonon description. Therefore, we will compare the present results with the available experimental data.

The experimental results reported to date[5-7] for γ in $GaAs/Al_xGa_{1-x}As$ systems are between 5.5 and 12 meV for well widths in the range 60–200 Å. Perhaps the most detailed results were given by Chen *et al.*,[6] who deconvolved the homogeneous and inhomogeneous linewidths, fitted the temperature dependence of the homogeneous linewidth to a form like that in Eq. (1.1) with the linear term omitted, and studied the linewidth as a function of well width.[28] They obtain a value for γ that decreases from 10.9 to 7.8 meV for well widths increasing from 60 to 200 Å. The overall magnitude of the damping obtained here and shown in Fig. 1 and its variation with the well widths in the range 60–200 Å is generally in good accord with those reported experimentally.[6]

As we mentioned in the Introduction, a more complete calculation would take into account the "polariton effect" in the evaluation of the linewidth. This feature results from the fact that the resonance between the exciton and light should be taken into account in the initial state.[10] The proper modes of the system then are polaritons.[29] Because the phonon couples only to the exciton component of the polariton, this results in a reduced value for the linewidth. In an earlier publication[11] we have investigated this effect for the bulk case and found a reduction factor of about 0.8 for GaAs. In the quantum-well case the calculation would be more complicated, and we have not carried it out. We would like to point out that in an earlier paper[15] we used a reduction factor of 0.5 for the "polariton effect." Based on our results for the bulk,[11] we now believe that this was an overestimate of the reduction and that the uncertainties in the present results for the quantum-well case, due to the neglect of the polariton effect, are comparable to those due to uncertainties in the band-structure parameters.

V. EFFECTS OF PHONON CONFINEMENT ON THE EXCITON LINEWIDTH

The results presented in Fig. 1 were derived assuming that the confined exciton interacts with 3D bulk LO phonons. As mentioned in the preceding section, more detailed calculations should include the effects of the interface on the vibrational modes. In quantum wells and superlattices the optical modes are usually classified as confined bulklike slab modes and interface modes.[30-33] There is a number of reviews on this subject, e.g., by Klein[30] and by Cardona.[31]

The electron-phonon interaction in a dielectric slab model[34] and its modifications for heterostructures[35] and superlattices[36] were discussed in Refs. 32–34 using electrical boundary conditions without regard to the atomic displacements at the interface. In this case, the electric potential for the bulklike slab modes has nodes at the interface, and their vibrational amplitudes are given by

$$W_{m+} \propto \sin(m\pi z/L), \quad m=1,3,5,\ldots$$
$$W_{m-} \propto \cos(m\pi z/L), \quad m=2,4,6,\ldots . \tag{5.1}$$

As discussed in Ref. 30, this description of the bulklike modes is acceptable only if the in-plane component of the polarization is much larger than its z component; this condition can be written in terms of the phonon wave vector as $q \gg \pi/L$, where q is the component of the wave vector parallel to the interface. The opposite limit, $q \ll \pi/L$, is realized in at least some Raman-scattering experiments.[30,31] For these cases it has been argued that the boundary condition that causes the electric potential to have nodes at the interfaces should be neglected in favor of the approximate boundary condition on the atomic displacements, in which case the electric field has nodes at the interfaces.[31] The vibrational amplitudes of the slab modes are then given by

$$W_{m+} \propto \sin(m\pi z/L), \quad m=2,4,6\ldots$$
$$W_{m-} \propto \cos(m\pi z/L), \quad m=1,3,5\ldots . \tag{5.2}$$

This representation is usually employed to analyze Raman-scattering data[32] and also to calculate electron scattering rates in quantum wells.[37]

The in-plane component q of the phonon wave vector that enters in Eq. (2.15), in general, can be comparable to π/L. In fact, with the parameters we used for the GaAs quantum well, qL varies from 0 to approximately 8 in Eq. (2.15). Thus, neither (5.1) nor (5.2) is applicable in our case. There exist a number of the microscopic model calculations (see, e.g., Ref. 38) for the confined modes. Here we employ the relatively simple model of Huang and Zhu.[39] They have given numerical solutions for their microscopic model and have also given convenient analytical approximations for their numerical solutions. Their model gives modes having both electric potential and polarization with nodes at the interfaces.

The electric potential can be written inside the layer as

$$V(r,z) \propto \Phi_m(z)\exp(i\mathbf{q}\cdot\mathbf{r}) , \tag{5.3}$$

where $\mathbf{r}$ and $\mathbf{q}$ are 2D vectors. When the electron and hole are each restricted to the first confined level of their corresponding potential wells as in Eq. (4.3), the only solutions to the model of Huang and Zhu[39] that couple to the carriers have a symmetric $\Phi_m(z)$. The analytical approximations for these modes are[39]

$$\Phi_m(z)=\cos(m\pi z/L)-(-1)^{m/2}, \quad m=2,4,6\ldots . \tag{5.4}$$

These functions are also exact solutions of the dielectric model which incorporates the boundary conditions on Φ and on W.[39] However, the solutions given by Eq. (5.4) are not an orthogonal set, and only the first few of them are approximately orthogonal for $qL/\pi \lesssim 1$. These first few modes, however, contribute most to the interaction of the exciton with the bulklike confined phonons in the evaluation of $\Gamma(T)$, and thus we use Eq. (5.4) as the best available analytical approximation for the confined phonon modes.

When the optical displacement is determined from Eqs. (5.3) and (5.4) by $w \propto -\nabla V(\mathbf{r},z)$ and properly nor-

malized,[39] we obtain for the electron-confined optical-phonon interaction the following matrix element:

$$u^{\mathrm{I}}_{m+}(q)=[4\pi e^2V^{-1}\hbar\omega_{\mathrm{LO}}(\epsilon_\infty^{-1}-\epsilon_0^{-1})]^{1/2}\times[\cos(\pi mz/L)-(-1)^{m/2}]\times[3q^2+(\pi mz/L)]^{-1/2}\ , \tag{5.5}$$

where q is an electron's in-plane momentum transfer given by the phonon's in-plane momentum. For comparison, if we use the solutions given by Eq. (5.2) we obtain

$$u^{\mathrm{II}}_{m+}(q)=[4\pi e^2V^{-1}\hbar\omega_{\mathrm{LO}}(\epsilon_\infty^{-1}-\epsilon_0^{-1})]^{1/2}\times\cos(\pi mz/L)[q^2+(\pi mz/L)^2]^{-1/2}\ . \tag{5.6}$$

In a quantum-well model with infinite barriers for carriers [Eq. (4.3)] only the $m=2$ mode of Eq. (5.2) couples to the electron and hole. That causes the results for Γ derived from Eq. (5.6) to be considerably smaller than those derived from the Huang and Zhu model [Eq. (5.5)].

Thus far we have discussed only the bulklike modes. The dielectric continuum model also predicts interface modes.[34–36] In a microscopic model,[39] if a dispersion of the bulk optical phonons is taken into account, these modes are partially mixed with the slab modes. In this work we treat bulk optical phonons as dispersionless and thus neglect the mode mixing. The interface modes have been studied experimentally by Raman scattering,[33,30,31] and it was found that the dielectric model gives a reasonably good approximation for them. To simplify the calculations, we shall use the interface modes obtained for a single quantum well[35] rather than those for the superlattice.[36] The corresponding electron-phonon interaction matrix element with the in-plane momentum transfer q is given by[35,36]

$$u(q)=(2\pi e^2f_\mu^2)^{1/2}(\hbar\omega_\mu Aq)^{-1/2}(1+e^{-qL})^{-1/2}\times(e^{-q(L/2-z)}+e^{-q(L/2+z)})\ , \tag{5.7}$$

where μ labels phonon modes. If bulk optical phonons are assumed to be dispersionless, there are only two different symmetric interface modes which we shall label $\mu=\pm$:

$$f^s_\pm=\pm\frac{(\hbar^2\omega_\pm^2-T_1^2)(\hbar^2\omega_\pm^2-T_2^2)}{\hbar^2(\omega_+^2-\omega_-^2)(\epsilon_1-\epsilon_2)}\ , \tag{5.8}$$

$$\epsilon_1=\epsilon_{\infty 1}(1-e^{-qL})\ , \tag{5.9}$$

$$\epsilon_2=\epsilon_{\infty 2}(1+e^{-qL})\ , \tag{5.10}$$

$$(\hbar\omega_\pm)^2=(\epsilon_1+\epsilon_2)^{-1}\times\{p\pm[p^2-(\epsilon_1+\epsilon_2)(\epsilon_1L_1^2T_2^2-\epsilon_2L_2^2T_1^2)]^{1/2}\}\ , \tag{5.11}$$

$$p=\tfrac{1}{2}[\epsilon_1(T_2^2+L_1^2)+\epsilon_2(T_1^2+L_2^2)]\ , \tag{5.12}$$

$$T_i=\hbar(\omega_{\mathrm{TO}})_i\ , \tag{5.13}$$

$$L_i=\hbar(\omega_{\mathrm{LO}})_i\ , \tag{5.14}$$

$$L_i^2/T_i^2=\epsilon_{0i}/\epsilon_{\infty i}\ , \tag{5.15}$$

where index i refers to the two different materials.

These interface modes are shown in Fig. 2 for the GaAs/AlAs system for dispersionless bulk optical phonons. We also neglect the bulk dispersion in calculations of the exciton linewidth $\Gamma(T)$ also.

The exciton intrasubband contribution $\Gamma_{1s,1s}$ is calculated with the separable variational wave functions of Eq. (4.8). The calculations are similar to those of Sec. IV except that now for the bulklike modes we sum over m instead of integrating over q. The contribution of the interface modes involves two different modes with different dispersions and, as a result, $\Gamma(T)$ cannot be written with a single-phonon occupation function as in Eq. (1.1). Thus in the presentation of the results for the L dependence of $\Gamma(T)$, we must choose a particular temperature.

As in Sec. IV we approximate

$$\Gamma_{1s}=\Gamma_{1s,1s}+\Gamma_{1s,\mathrm{cont}}\ , \tag{5.16}$$

and each of these contributions is further written as

$$\Gamma_{1s,i}=\Gamma^b_{1s,i}+\Gamma^+_{1s,i}+\Gamma^-_{1s,i}\ , \tag{5.17}$$

where the first term on the right represents the contribution of the bulklike confined modes, and the last two terms represent contributions of the interface modes. Because the calculations are a straightforward generalization of those of Sec. IV, we omit the details here.

The results for $\Gamma(T)$ obtained from the exciton-phonon interaction from Eqs. (5.5) (with $m\leq 8$ terms taken into account) and (5.7) are shown in Fig. 3 as a function of L for $T=200$ K. For comparison we also give results for $\Gamma(T)$ calculated using 3D phonons and a separable approximation for the exciton states. We also show in Fig.

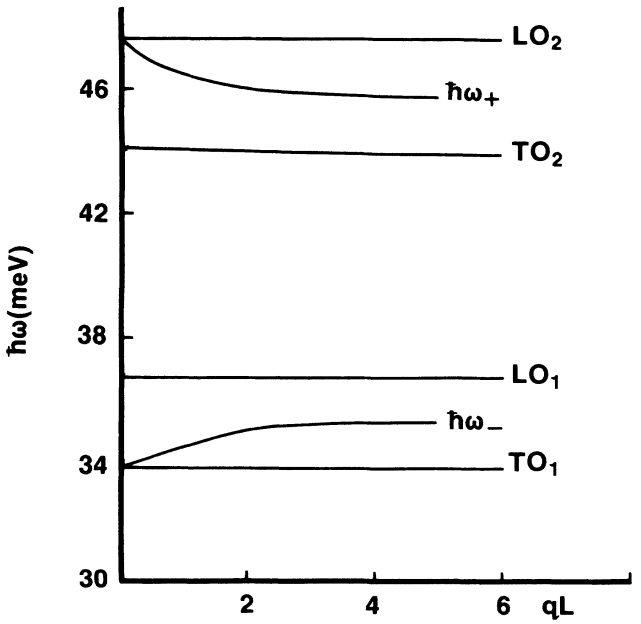

FIG. 2. $\hbar\omega_+$ and $\hbar\omega_-$ are the energies of the interface phonons in a GaAS/AlAs quantum-well structure as obtained from Eq. (5.11). The bulk optical modes are assumed to be dispersionless, and we use the following values for the material parameters: for GaAs, $\epsilon_{01}=12.35$, $\epsilon_{001}=10.48$, $\hbar\omega_{\mathrm{LO}}=36.8$ meV, $\hbar\omega_{\mathrm{TO}}=34.0$ meV; for AlAs, $\epsilon_{02}=10.0$, $\epsilon_{002}=8.16$, $\hbar\omega_{\mathrm{LO}}=47.7$ meV, $\hbar\omega_{\mathrm{TO}}=44.0$ meV.

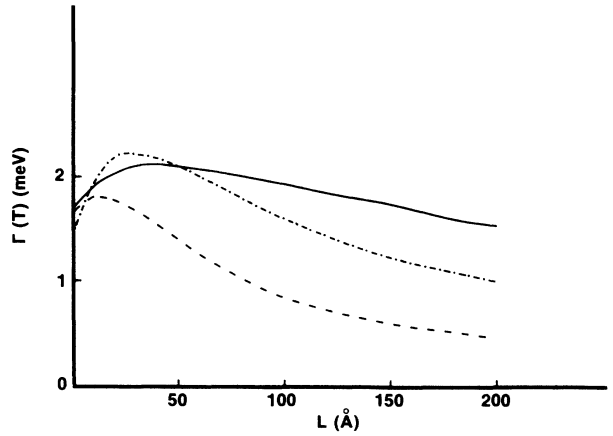

FIG. 3. Results obtained for the optical-phonon-induced linewidth $\Gamma(T)$ for excitons in a quantum well as a function of well width L at temperature $T=200$ K taking phonon confinement into account. Both the bulklike confined phonon modes and the interface phonon modes are included. The solid curve is obtained using the model of Huang and Zhu (Ref. 37) for the bulklike slab modes, and the dashed curve is obtained using Eq. (5.2) for the bulklike modes. The effective mass of the heavy hole, m_h, equals $0.15m_0$ here. The dashed-dotted curve was obtained using a three-dimensional description of the LO phonons and taking a separable approximation for the exciton wave function in the evaluation of both intraband $(1s,1s)$ and interband $(1s,\text{cont})$ contributions.

3 the results for $\Gamma(T)$ which were obtained using Eq. (5.2) for the bulklike modes. As discussed in the preceding section, we believe that this last model underestimates the exciton linewidth.

We find that taking phonon confinement into account using a relatively simple model based on the microscopic model of Huang and Zhu, which incorporates boundary conditions on both the electric potential and optical displacement,[39] gives $\Gamma(T)$ which is fairly close to that obtained using a 3D-phonon description. We find that the exciton lifetime resulting from this model has a weaker dependence on the well width L than those based on the other models studied here. The similarity of the results for this model and those based on the 3D-phonon description tends to justify our comparison of the latter with the available experimental data in Sec. IV.

VI. SUMMARY

We have presented a detailed treatment of the LO-phonon-induced exciton linewidth in a semiconductor quantum well. For electrons and heavy holes confined in their lowest quantum-well subbands, the complete summations over all intermediate exciton states have been included. The effects of the optical-phonon confinement also were studied in the present work. Results for the exciton linewidths were found to be in general agreement with experiment.

ACKNOWLEDGMENTS

This work was supported in part by the Office of Naval Research (T.L.R.).

APPENDIX

Quantity $\Delta(n,n)$ in Eq. (3.34) is given by

$$\Delta(n,n_1)=|v(n,n_1)|^2(2aq_n)^{-1}\ , \tag{A1}$$

where

$$q_n=(2M/\hbar^2)^{1/2}[W_0+R(n+\tfrac{1}{2})^{-2}]^{1/2}\ , \tag{A2}$$

$$R=\mu e^4/2\epsilon_0\hbar^2\ , \tag{A3}$$

$$W_0=\omega_{\rm LO}\hbar-4R\ , \tag{A4}$$

$$\begin{aligned}|v(n,n_1)|^2=&16c(n,n_1)\\&\times\{t_1^2r_1^{2(n-1)}R_1^2+t_2^2r_2^{2(n-1)}R_2^2\\&-2t_1t_2(r_1r_2)^{n-1}R_1R_2\\&\times\cos[(n_1-n_2)(\alpha_1-\alpha_2)-(\delta_1-\delta_2)]\}\ ,\end{aligned} \tag{A5}$$

where $n_2=n-n_1$,

$$c(0,0)=1\ , \tag{A6}$$

$$\begin{aligned}c(n,n)&=c(n,0)\\&=(2n+1)^{-4}(1+\tfrac{1}{2})\times\cdots\times(1+1/2n)\ .\end{aligned} \tag{A7}$$

For $n\geq 1$ and $n_1<n$,

$$\begin{aligned}c(n,n_1)=&(2n+1)^{-3}(2n_1+1)^{-1}(2n_2+1)^{-1}\\&\times(1+\tfrac{1}{2})\times\cdots\times(1+1/2n_1)(1+\tfrac{1}{2})\\&\times\cdots\times(1+1/2n_2)\ ,\end{aligned} \tag{A8}$$

$$r_i^2=\frac{(1+1/2n)^{-2}+Q_i^2a^2}{(1+1/n)^2(1+1/2n)^{-2}+Q_i^2a^2}\ , \tag{A9}$$

$$t_i^2=[(1+1/n)^2(1+1/2n)^{-2}+Q_i^2a^2]^{-1}\ , \tag{A10}$$

$$\begin{aligned}\tan\alpha_i=&Q_ia(n+\tfrac{1}{2})^{-1}\\&\times[(1+1/n)(1+1/2n)^{-2}+Q_i^2a^2]^{-1}\ ,\end{aligned} \tag{A11}$$

$$R_i^2=[(n+1)r_i\cos\beta_i-n\cos(\alpha_i+\beta_i)]^2 \tag{A12}$$

$$+(n_1-n_2)^2[r\sin\beta-\sin(\alpha+\beta)]^2\ , \tag{A13}$$

$$\tan\beta_i=Q_ia(1+1/2n)(1+1/n)^{-1}\ , \tag{A14}$$

$$\tan\delta_i=\frac{(n_1-n_2)[r_i\sin\beta_i-\sin(\alpha_i+\beta_i)]}{(n+1)r\cos\beta-n\cos(\alpha_i+\beta_i)}\ . \tag{A15}$$

Q_i is defined in Eq. (3.29); index i here labels electron $(i=1)$ and hole $(i=2)$.

At large n, $\Delta(n,n_1)$ is $O(n^{-3})$, and this provides reasonably fast convergence in Eq. (3.34).

Next, we write the following expressions for the functions F_{ee}, F_{hh}, and F_{eh} that appear in Eq. (3.35):

$$F_{ee}(x)=(r_1g_1)^{-5}(m_e/m_h)^2y(2S_1^2+x^2+4)\ , \tag{A16}$$

$$F_{hh}(x)=(r_2g_2)^{-5}(m_h/m_e)^2y(2S_2^2+x^2+4)\ , \tag{A17}$$

$$y^2=x_0^2-x^2\ , \tag{A18}$$

$$r_i^2=1+(S_i+x)^2 , \tag{A19}$$

$$g_i^2=1+(S_i-x)^2 , \tag{A20}$$

$$S_1=ym_e/m_h , \tag{A21}$$

$$S_2=-ym_h/m_e , \tag{A22}$$

$$F_{eh}=(2/\pi)\exp(\pi/2x)S_1S_2(r_1r_2g_1g_2)^{-5/2} \times[S_1S_2J_1-2(S_1+S_2)J_2-4J_3] \times\cos(\delta_1-d/2x)\exp(-\delta_2/x) , \tag{A23}$$

$$d=\ln(r_1g_2/r_2g_1) , \tag{A24}$$

$$\tan\phi_i^{\pm}=x\pm Q_i , \tag{A25}$$

$$\delta_1=\phi_1^+ +\phi_1^- -\phi_2^+ -\phi_2^- , \tag{A26}$$

$$\delta_2=\phi_1^+ +\phi_1^- +\phi_2^+ +\phi_2^- . \tag{A27}$$

Defining $u=\cosh d$,

$$F_1(x)={}_2F_1(i/2x+\tfrac{1}{2},-i/2x+\tfrac{1}{2},1,(1-u)/2) , \tag{A28}$$

$$F_2(x)={}_2F_1(i/2x+\tfrac{3}{2},-i/2x+\tfrac{3}{2},2,(1-u)/2) , \tag{A29}$$

$$F_3(x)={}_2F_1(i/2x+\tfrac{5}{2},-i/2x+\tfrac{5}{2},3,(1-u)/2) , \tag{A30}$$

where ${}_2F_1$ is a hypergeometric function. The functions J_1,J_2,J_3 that appear in Eq. (A23) are

$$J_1=\pi[\cosh(\pi/2x)]^{-1}F_1(x) , \tag{A31}$$

$$J_2=-(\pi/8)[\cosh(\pi/2x)]^{-1} \times(1+x^2)(u^2-1)^{1/2}F_2(x) , \tag{A32}$$

$$J_3=-(\pi/8)[\cosh(\pi/2x)]^{-1}(1+x^2) \times[xuF_2(x)-(1+9x^2)(u^2-1)(16x)^{-1}F_3(x)] . \tag{A33}$$

These equations are used to evaluate J_1, J_2, and J_3 by series expansion in powers of $1-u$ for $x\le 1$. For $1\le x\le x_0$ we evaluate these functions via their integral representations:

$$J_1=4I_1 , \tag{A34}$$

$$J_2=-4(u^2-1)^{1/2}I_2 , \tag{A35}$$

$$J_3=-4u[I_2-3(u^2-1)^{1/2}I_3] , \tag{A36}$$

where

$$I_1(x)=\int_0^{\infty}dz\,e^{-z}\cos(z/x)(1+2u+e^{-4z})^{-1/2} , \tag{A37}$$

$$I_2(x)=\int_0^{\infty}dz\,e^{-z}\cos(z/x)(1+2u+e^{-4z})^{-3/2} , \tag{A38}$$

$$I_3(x)=\int_0^{\infty}dz\,e^{-z}\cos(z/x)(1+2u+e^{-4z})^{-5/2} . \tag{A39}$$

[1]See, e.g., M. Jaros, *Physics and Applications of Semiconductor Microstructures* (Oxford University Press, Oxford, 1989).

[2]R. C. Miller, D. A. Kleinman, W. T. Tsang, and A. C. Gossard, Phys. Rev. B **24**, 1134 (1981).

[3]D. A. B. Miller, D. S. Chemla, D. J. Eilenberger, P. W. Smith, A. C. Gossard, and W. Wiegmann, Appl. Phys. Lett. **42**, 925 (1983).

[4]D. A. B. Miller, Opt. Eng. **26**, 368 (1987); D. A. B. Miller, J. E. Henry, A. C. Gossard, and J. H. English, Appl. Phys. Lett. **49**, 821 (1986).

[5]D. C. Chemla, D. A. B. Miller, P. W. Smith, A. C. Gossard, and W. Wiegmann, IEEE J. Quantum Electron. **QE-20**, 265 (1984).

[6]Y. Chen, G. P. Kothiyal, J. Singh, and P. K. Bhattacharya, Supperlatt. Microstruct. **3**, 657 (1987).

[7]O. J. Glembocki, B. V. Shanabrook, and W. T. Beard, Surf. Sci. **174**, 201 (1985).

[8]B. H. Iwamura, H. Kobayashi, and H. Okamota, Jpn. J. Appl. Phys. **23**, L795 (1984).

[9]J. Lee, E. S. Koteles, and M. O. Vassel, Phys. Rev. B **33**, 5512 (1986).

[10]B. Segall, in *Proceedings of the IXth International Conference on the Physics of Semiconductors, Moscow, 1968* (Nauka, Leningrad, 1968), p. 425.

[11]S. Rudin, T. L. Reinecke, and B. Segall (unpublished).

[12]B. Segall and G. D. Mahan, Phys. Rev. **171**, 935 (1968).

[13]Y. Toyozawa, Prog. Theor. Phys. **20**, 53 (1958); J. Phys. Chem. Solids **25**, 59 (1964).

[14]H. N. Spector, J. Lee, and P. Melman, Phys. Rev. B **34**, 2554 (1986).

[15]S. Rudin and T. L. Reinecke, Supperlatt. Microstruct. **3**, 137 (1987).

[16]G. Bastard, E. E. Mendez, L. L. Chang, and L. Esaki, Phys. Rev. B **26**, 1974 (1982).

[17]J. M. Luttinger and W. Kohn, Phys. Rev. **97**, 869 (1955).

[18]G. Dresselhouse, Phys. Chem. Soilds **1**, 14 (1956).

[19]W. Kohn, Phys. Chem. Solids **8**, 45 (1959); Phys. Rev. **110**, 857 (1958); **105**, 509 (1957).

[20]H. Haken, in *Polarons and Excitons,* edited by C. G. Kuper and G. D. Whitfield (Plenum, New York, 1963), p. 295.

[21]Effect of the image charges on the exciton binding energies recently was calculated by D. M. Whittaker and R. J. Elliott, Solid State Commun. **68**, 1 (1988). They find about 10% change of the exciton binding energy in 60–100-Å-wide $GaAs/Al_xGa_{1-x}As$ quantum wells.

[22]E. Hanamura and H. Haug, Phys. Rep. **33C**, 211 (1977).

[23]P. M. Morse and H. Feshbach, *Methods of Theoretical Physics* (McGraw-Hill, New York, 1953).

[24]L. D. Landau and E. M. Lifshitz, *Quantum Mechanics—Nonrelativistic Theory* (Pergamon, London, 1965).

[25]D. A. Broido, Ph.D. thesis, University of California, San Diego, 1985, and private communication.

[26]Y. Shinozuka and M. Matsuura, Phys. Rev. B **28**, 4878 (1983); **29**, 3717(E) (1984).

[27]The present results for $m_h=0.3m_0$ can be compared to the theoretical results of Refs. 9 and 14 in which the plane-wave aproximation was used for the electron-hole scattering states. The total value of the linewidth parameter γ obtained in Ref. 9 is about one-half of that calculated here. Although we should expect the total γ to be different, the intraband contribution $\gamma(1s,1s)$ should be the same in the 2D limit $L=0$. However, this quantity in Ref. 14 [their Eq. (28)] is twice as

large as ours. We do not know the reason for this discrepancy and can only assume that it is related to their definition of the linewidth.

[28]The authors of Ref. 6 do not include a term corresponding to acoustic phonons in fitting their experimental data. Because the optical-phonon contribution dominates for $T > 200$ K (Ref. 9), the value for the phonon-induced linewidth in Ref. 6 is obtained primarily from their high-temperature data and probably is reliable.

[29]J. J. Hopfield, Phys. Rev. **112**, 1555 (1958).

[30]M. V. Klein, IEEE J. Quantum Electron. **QE-22**, 1760 (1986).

[31]M. Cardona, in *Lectures on Surface Science,* edited by G. R. Castro and M. Cardona (Springer-Verlag, Berlin, 1987).

[32]A. K. Sood, J. Menendez, M. Cardona, and K. Ploog, Phys. Rev. Lett. **54**, 2111 (1985); Phys. Rev. **32**, 1412 (1985).

[33]A. K. Sood, J. Menendez, M. Cardona, and K. Ploog, Phys. Rev. Lett. **54**, 2115 (1985).

[34]J. J. Licari and R. Evrard, Phys. Rev. B **15**, 2254 (1977).

[35]R. Lassnig, Phys. Rev. B **30**, 7132 (1984).

[36]E. P. Pokatilov and S. I. Beril, Phys. Status Solidi B **118**, 567 (1983).

[37]B. K. Ridley, Phys. Rev. B **39**, 5282 (1989).

[38]G. Kanellis, J. F. Morhange, and M. Balkanski, Phys. Rev. B **28**, 3406 (1983).

[39]K. Huang and B. Zhu, Phys. Rev. B **38**, 2183 (1988); **38**, 13 377 (1988).